

Studies of the Solid/Solution “Interfacial” Dealumination of Kaolinite in HCl(aq) Using Solid-State ^1H CRAMPS and SP/MAS ^{29}Si NMR Spectroscopy

John J. Fitzgerald,^{*,†} Abdullatef I. Hamza,[†] Charles E. Bronnimann,^{‡,§} and Steven F. Dec^{‡,||}

Contribution from the Department of Chemistry, South Dakota State University, Brookings, South Dakota 57007, and Department of Chemistry, Colorado State University, Fort Collins, Colorado 80523

Received January 27, 1997. Revised Manuscript Received April 18, 1997[⊗]

Abstract: The dealumination of kaolinite by the solid/solution “interfacial” reaction with HCl(aq) at 98 °C was investigated using solid-state ^1H CRAMPS and MAS ^{29}Si NMR techniques. The single-pulse (SP)/MAS ^{29}Si NMR spectra of kaolinite-derived solids that are 2–83% dealuminated are observed to be dependent upon the degree of dealumination, showing three resolvable resonances at –89, –100, and –109 ppm. The –89 ppm resonance is due to silicon Q³-type Si(OSi)₃(OAl)₂ sites in unreacted kaolinite, while the latter two resonances are assigned to new Q³-type silica–alumina (Si–OH⁺–Al) and to Q⁴-type amorphous silica (Si(OSi)₄) sites contained in dealuminated kaolinite solids following partial dealumination. The ^1H CRAMPS spectra of these dealuminated solids are also dependent upon the degree of removal of Al³⁺ ions from the kaolinite Al–OH–Al layer. In addition to a broad proton peak at 4.0 ppm due to structural protons of the intact Al–OH–Al layer in unreacted kaolinite, two new resonances at 0.4 and 7.0 ppm are assigned to protons of the new silanol (Si–OH) and alumina–silica (Si–OH⁺–Al) sites. The spectral intensities of the SP/MAS ^{29}Si and ^1H CRAMPS NMR results are correlated with the progress of dealumination, permitting the development of a structural model for partially dealuminated kaolinite. This structural model is consistent with a kinetic model involving a chemically-controlled “heterogeneous” reaction process whereby H⁺ ion attack of the Si–O–Al linkages at the edges of the mineral surface leads to liberation of aluminum ions into the solution medium.

Introduction

Reactions of clay minerals in the solid state and at the solid/solution interface are of fundamental significance in materials science. The mineral kaolinite, Al₂Si₂O₁₀(OH)₂, is the major constituent of kaolin and is an important type of dioctahedral 1:1 layered aluminosilicate clay.^{1,2} These materials have found extensive use as fillers and pigment coatings,³ precursors for the synthesis and production of zeolites^{4,5} and ceramic materials,⁶ and acidic Si/Al catalysts in organic synthesis and large-scale industrial processes.^{7–10}

Numerous studies have been reported for three major solid-state and solid/solution “interfacial” reactions important in producing kaolin-derived materials: (1) the dehydration of kaolinite to metakaolinite from 150 to 650 °C,^{11–22} (2) the high-temperature (>980 °C) transformation of metakaolinite to γ -alumina, mullite (an alumina–silica), and amorphous silica-phase mixtures,^{11,13–16,18–23} and (3) the dealumination of un-

* Author to whom correspondence should be addressed.

[†] South Dakota State University.

[‡] Colorado State University.

[§] New address: Otsuka Electronics, Fort Collins, CO 80523.

^{||} New address: Department of Chemistry, Colorado School of Mines and Technology, Golden, CO.

[⊗] Abstract published in *Advance ACS Abstracts*, July 1, 1997.

(1) Brown, G. *Phil. Trans. R. Soc. Lond.* **1984**, A311, 221.

(2) Bailey, S. W. *Crystal Structure of Clay Minerals and Their X-Ray Identification*; Brindley, G. W.; Brown, G., Eds.; Mineralogical Society Monograph No. 5; Mineralogical Society: London, 1980; p 28.

(3) Jepsen, W. B. *Phil. Trans R. Soc. Lond.* **1984**, A311, 411.

(4) Barrer, R. M. *Hydrothermal Chemistry of Zeolites*; Academic Press: London, 1982; 216. See also: Barrer, R. M. *Zeolites and Clay Minerals, Sorbents and Molecular Sieves*; Academic Press: New York, 1978.

(5) Breck, R. M. *Zeolite Molecular Sieves: Structure, Chemistry and Use*; Wiley & Sons: New York, 1974; p 731.

(6) Ryan, W. *Properties of Ceramic Raw Materials*; Pergamon Press: Oxford, 1978.

(7) Barrer, R. M.; Cole, J. F.; Sticker, H. U.S. Patent 3,663,164, 1982.

(8) Plank, C. J.; Rosinski, E. J. U.S. Patent 3,676,330, 1982.

(9) Nealong, E. J.; Maher, P. K. Canadian Patent 755,549, 1963.

(10) Laszlo, P. *Science* **1987**, 234, 1473. Haddix, G. W.; Narayana, M. NMR of Layered Materials for Heterogeneous Catalysis. In *NMR Techniques in Catalysis*; Bell, A. T.; Pines, A., Eds.; Marcel Dekker, Inc.: New York, 1994; pp 312–333.

(11) Brindley, G. B.; Nakahira. *J. Am. Ceram. Soc.* **1959**, 42(7), 319.

(12) Brindley, G. B.; Nakahira. *J. Am. Ceram. Soc.* **1959**, 42(7), 314.

(13) Chakraborty, A. K.; Ghosh, D. K. *J. Am. Ceram. Soc.* **1978**, 3–4, 170.

(14) Okado, K.; Otsuka, N.; Otsuka, J. *J. Am. Ceram. Soc.* **1986**, 69(10), C251.

(15) Komarneni, S.; Fyfe, C. A.; Kenedy, G. J. *Clay Miner.* **1985**, 20, 327.

(16) Meinhold, R. H.; MacKenzie, K. J. D.; Brown, I. W. M. *J. Mater. Sci. Lett.* **1985**, 4, 163.

(17) MacKenzie, K. J. D.; Brown, I. W. N.; Meinhold, R. H.; Bowden, M. E. *J. Am. Ceram. Soc.* **1985**, 68, 293.

(18) Watanabe, T.; Shimizu, T.; Nagasawa, K.; Masuda, A.; Saito, H. *Clay Miner.* **1987**, 22(1), 37.

(19) Lambert, J. F.; Millman, W. S.; Fripiat, J. J. *J. Am. Chem. Soc.* **1989**, 111, 3517.

(20) Sanz, J.; Madani, A.; Serratos, J. M.; Moya, J. S.; Aza, S. *J. Am. Ceram. Soc.* **1988**, 71(10), C418.

(21) Brown, I. W. M.; MacKenzie, K. J. D.; Bowden, M. E.; Meinhold, R. H. *J. Am. Chem. Soc.* **1985**, 68, 298.

(22) Jocha, J.; Klinowski, J. *Phys. Chem. Mineral* **1990**, 17, 179.

(23) Jocha, J.; Klinowski, J. *Angew. Chem., Int. Ed. Engl.* **1990**, 29, 553.

(24) Tilley, G. S.; Miller, R. W.; Ralston, O. C. U.S. Bureau of Mines, Dept. of Interior, Report RI 8978, 1985.

(25) Pask, J. A.; Davis, B. U.S. Bureau of Mines, Technical Paper 664, 1945, pp 661–687.

(26) Carroll, D.; Starkey, H. C. *Clay Miner.* **1971**, 19(5), 321.

(27) Mitra, N. K.; Das Poddar, P. K.; Mandal, R. K. *J. Aust. Ceram. Soc.* **1981**, 17(2), 52.

(28) Bengtson, K. B. *Am. Inst. Min. Metal Pet. Eng. Light Metals* **1979**, 1, 217.

calcined and calcined kaolinite by solid/solution reactions with aqueous acids at elevated temperature.^{29–31}

While classical studies have described the solid-state thermal conversions of kaolinite using X-ray diffraction (XRD) and differential thermal analysis (DTA) approaches, recent high-resolution magic-angle spinning (MAS) ²⁷Al and ²⁹Si NMR studies have been reported for the solid-state dehydroxylation of kaolinite to metakaolinite between 150 and 650 °C^{10–15} and the high-temperature (>980 °C) conversion of metakaolinite to mixtures of γ -alumina, mullite, and amorphous silica.^{15,16,18–23} The formation of metakaolinite occurs without disruption of the Si–O–Al linkage based on ²⁹Si NMR, while ²⁷Al NMR evidence indicates that major structural changes convert the six-coordinate aluminums in kaolinite into mixtures of 4-, 5-, and 6-coordinate aluminums in metakaolinite.^{17,19–22} The corresponding ²⁹Si MAS NMR shows spectral changes consistent with increases in the Si–O–Si bond angles as the silica layer becomes disordered due to the major structural reorganization in the attached alumina layer.^{16,18–23} ²⁷Al NMR results have shown that heating metakaolinite above 850 °C leads to the formation of γ -alumina (containing 4- and 6-coordinate aluminums) as the Si–O–Al linkage ruptures during phase separation into an alumina-rich and silica-rich phase. At higher temperatures, both ²⁷Al and ²⁹Si NMR indicate the formation of mullite and cristobalite.^{18–23}

The solid/solution dealumination reaction of calcined and kaolinite materials in acidic aqueous media has also been extensively investigated by classical chemical analysis^{21–31} and kinetic approaches.^{32,33} Bengston²⁸ and Bremmer *et al.*²⁹ showed that extraction of aluminum from calcined kaolinitic clays by aqueous HCl is the most favorable approach to obtain alumina materials from nonbauxitic minerals. Alternatively, other workers have utilized this reaction to prepare acidic Si/Al catalytic materials using both calcined and natural kaolinite.^{10,24,30} While kaolin materials calcined between 500 and 850 °C are readily dealuminated in HCl(aq), natural kaolinite is resistant to acid attack, undergoing dealumination very slowly.^{24–26,28} Kinetic studies of the HCl(aq) dealumination of kaolinite by Miller³² showed that the reaction in excess acid conditions obeys pseudo-zero-order kinetics with respect to aluminum for the release of aluminum and may involve a “heterogeneous” chemically-controlled edge attack by hydrogen ion. Similar studies of the dealumination of montmorillonite, a 2:1 Si/Al clay, indicate that the related reaction is also a chemically-controlled process but involves an all-surface or “homogeneous” H⁺ ion attack.^{32,34} Langston and Jenne³⁵ and Miller³² concluded that these clay/HCl(aq) “interfacial” reactions display different reaction kinetics that depend upon the structural characteristics of the specific clay minerals. Recent studies by Malybaeva³³ concluded that the mechanism of reaction of HCl(aq) with various alumina-containing materials involves diffusion of H⁺ ion to the reactive mineral sites, chemical reaction at the phase boundary where the Si–O–Al interface is disrupted, and mass transfer of the reaction products to the solution medium.

Multinuclear NMR techniques such as SP/MAS and CP/MAS ²⁹Si NMR and high-speed SP/MAS ²⁷Al NMR, in combination with ¹H CRAMPS techniques, provide unique capabilities to study the solid/solution “interfacial” reactions of clay minerals such as kaolinite and related layered inorganic materials. While MAS ²⁷Al and ²⁹Si NMR has been widely reported to study the solid-state reactions of clay minerals,^{18–23} the application of solid-state ¹H MAS NMR and CRAMPS (combined rotation and multiple-pulse spectroscopy) techniques to study clay minerals and their reactions has gone largely unexplored. Recent ¹H CRAMPS studies by Bronnimann *et al.*^{36–38} have examined the dehydration of silica–aluminas and silica gels. Dehydrated silica–aluminas exhibit three sharp proton NMR peaks at 7.0, 3.1, and 2.0 ppm assigned to proton-containing Si/Al Brønsted sites, “physisorbed” water, and Si–OH moieties in either silica gel or silica-like regions.³⁶ In addition, a broad 4.8 ppm proton NMR peak assigned to H₂O physisorbed on γ -alumina or alumina-like regions of the silica–aluminas has been observed. For silica gels of different stages of hydration, three resolvable ¹H CRAMPS peaks have also been observed.³⁷ The two sharp NMR peaks at 1.7 and 3.5 ppm are due to “isolated” non-H-bonded silanols and “physisorbed” water, respectively, and the broad 3.0 ppm peak is due to H-bonded Si–OH moieties. Characterization of hydrous species in minerals by ¹H CRAMPS techniques has not been reported, although Yesinowski *et al.*³⁹ reported high-speed MAS ¹H NMR for a range of minerals containing mobile, isolated, and structural waters and stoichiometric OH groups.³⁹

In this work, SP/MAS ²⁹Si NMR and ¹H CRAMPS investigations are reported for various dealuminated kaolinite solids obtained from the solid/solution “interfacial” reaction of kaolinite with aqueous 3 M HCl at 98 °C. MAS ²⁷Al NMR investigations³¹ of dealuminated kaolinite solids show that ²⁷Al NMR can be quantitatively correlated with the degree of dealumination or removal of aluminum from kaolinite and that no significant structural changes occur in the remaining aluminum contained in the intact gibbsite-like aluminum hydroxide layer of kaolinite following partial dealumination up to 83%. CP/MAS ²⁹Si NMR measurements of these partially dealuminated kaolinite solids, however, are observed to be dependent upon the degree of dealumination, exhibiting three peaks at –89, –99, and –100 ppm.³¹ The ²⁹Si NMR peak at –89 ppm was assigned to silicon sites of unreacted kaolinite, whereas the new ²⁹Si NMR peaks at –99 and –109 ppm were assigned to silicon atom sites where their local chemical environments are substantially altered following removal of aluminums from the nearby aluminum hydroxide layer.

The work described herein has been directed toward obtaining a more detailed understanding of the chemical and structural nature and interrelationship of the silicon and hydrogen sites in dealuminated kaolinite solids. The SP/MAS ²⁹Si NMR and ¹H CRAMPS studies have permitted the development of a structural model for dealuminated kaolinite materials. On the basis of this structural model and kinetic results reported here, a reaction mechanism for the dealumination of kaolinite by the solid/solution “interfacial” reaction with aqueous HCl is proposed. These results demonstrate the advantage of the simultaneous use of solid-state ¹H CRAMPS and ²⁹Si NMR techniques and

(29) Bremmer, P. R.; Nicks, L. H.; Bauer, D. J. U.S. Bureau of Mines, Dept. of Interior Report RI 8866, 1984.

(30) Sawyer, D. L.; Turner, T. L. U.S. Bureau of Mines, Dept. of Interior Report RI 8978, 1985.

(31) Fitzgerald, J. J.; Hamza, A. I.; Bronnimann, C. E.; Dec, S. F. *Solid State Ionics* **1989**, 32/33, 378.

(32) Miller, R. J. *Soil Sci. Soc. Am. Proc.* **1965**, 29, 36.

(33) Malybaeva, G. O.; Romanov, L. G.; Nurkeev, S. S. *Izo. Vyssh. Uchebn. Zaved. Tsvetn. Metall.* **1987**, 1, 50.

(34) Osthaus, B. *Natl. Acad. Sci. Pub.* **1956**, 456, 301.

(35) Langston, R. B.; Jenne, E. A. *Proc. 12th National Clay Conf.*; Pergamon Press: New York, 1964; pp 633–647.

(36) Bronnimann, C. E.; Chuang, I.-S.; Hawkins, B. L.; Maciel, G. E. *J. Am. Chem. Soc.* **1987**, 109, 1562.

(37) Bronnimann, C. E.; Zeigler, R. C.; Maciel, G. E. *J. Am. Chem. Soc.* **1988**, 110, 2023.

(38) Bronnimann, C. E.; Hawkins, B. L.; Zhang, M.; Maciel, G. E. *J. Am. Chem. Soc.* **1988**, 60, 1743.

(39) Yesinowski, J. P.; Eckert, H.; Rossman, G. R. *J. Am. Chem. Soc.* **1988**, 110, 1367.

Table 1. Solid-State SP/MAS ²⁹Si NMR Parameters for Dealuminated Kaolinite Solids

HCl extraction time (h)	% dealumination	% Al in solid	% Si* (−89 and −99 ppm peak)	δ(²⁹ Si) chemical shifts, ppm (rel peak intensity) ^a		
0	0.0	100.0	100 (100 + 0)	−89.1 (100)		
4	1.8	98.2	96 (96 + 0)	−89.0 (96)		−108.0 (4)
24	17.6	82.4	78 (63 + 15)	−90.8 (63)	−101.6 (15)	−112.2 (22)
48	38.3	61.7	56 (45 + 11)	−90.9 (45)	−99.2 (11)	−110.8 (44)
96	60.9	39.1	40 (22 + 18)	−89.2 (22)	−100.2 (18)	−108.5 (60)
192 (8 days)	72.3	27.7	28 (12 + 16)	−89.7 (12)	−99.8 (16)	−108.2 (72)
384 (16 days)	83.3	16.7	22 (6 + 16)	−90.7 (6)	−100.8 (16)	−110.8 (78)

^a Chemical shifts are relative to TTMSM. Relative peak intensities obtained from deconvolution analysis.

Table 2. Kinetic Parameters for Reaction of Kaolinite with Aqueous HCl under Various Conditions^a

experimental rate constants ^b		experimental reaction conditions				
<i>K'</i> (h ^{−1})	<i>k_s</i> (cm h ^{−1})	particle size range, μm	avg radius (<i>r_o</i>), cm	[HCl], M	<i>T</i> (°C)	
1.43 × 10 ^{−3}	8.33 × 10 ^{−5}	37 × 74	6.81 × 10 ^{−2}	3.0	98	
1.84 × 10 ^{−3}	3.56 × 10 ^{−5}	74 × 149	2.91 × 10 ^{−2}	3.0	98	
2.12 × 10 ^{−3}	1.38 × 10 ^{−5}	149 × 500	1.13 × 10 ^{−2}	3.0	98	
2.56 × 10 ^{−3}	7.64 × 10 ^{−6}	500 × 841	0.62 × 10 ^{−2}	3.0	98	
5.04 × 10 ^{−4}	5.75 × 10 ^{−5}	149 × 500	1.13 × 10 ^{−2}	1.0	98	
1.48 × 10 ^{−3}	2.34 × 10 ^{−5}	149 × 500	1.13 × 10 ^{−2}	2.0	98	
2.12 × 10 ^{−3}	1.38 × 10 ^{−5}	149 × 500	1.13 × 10 ^{−2}	3.0	98	
5.04 × 10 ^{−4}	3.44 × 10 ^{−6}	149 × 500	1.13 × 10 ^{−2}	3.0	70	
7.88 × 10 ^{−4}	7.44 × 10 ^{−6}	149 × 500	1.13 × 10 ^{−2}	3.0	85	
2.12 × 10 ^{−3}	1.38 × 10 ^{−5}	149 × 500	1.13 × 10 ^{−2}	3.0	98	

^a Reactions at stirring rates of 400 rpm. ^b Based on the chemically-controlled rate law expression eq 4, where *r_o* is given above, *V* = 3.05 × 10² cm²/mol, *b* = 12/1, and *n* = 1.3.

kinetic methods to examine solid/solution "interfacial" reaction processes that are important in clay mineral-based materials science.

Experimental Section

Preparation of Kaolinite-Derived Solids. The series of kaolinite-derived solids studied were obtained from reaction of 3 M HCl(aq) with kaolinite for time periods up to 16 days at 98 °C as previously described.³¹ Chemical analyses of the resulting solids, including % Si, % Al, and % Fe contents, percent weight loss, and powder XRD measurements, have also been reported.³¹

Experimental Kinetic Studies. The kinetic studies of dealumination used kaolinite obtained from D. J. Mineral Kit Co., Butte, MT (Lot M-188 from Lewiston, MT). Samples were ground with mortar and pestle and sieved using standard techniques into four particle size ranges: 37 × 74, 74 × 149, 149 × 500, and 500 × 841 μm. The kaolinite samples were reacted for up to 384 h by refluxing in aqueous 1, 2, and 3 M HCl at 95–98 °C with stirring at a HCl/kaolinite stoichiometry of 12/1. At selected times, aliquot samples were obtained and diluted with atomic absorption (AA) addition reagents, and the percent aluminum extracted was determined by AA analysis as described elsewhere.³¹ The rate of liberation of aluminum by extraction at 200, 400, and 600 rpm was independent of stirring rate up to 48 h. Further kinetic runs were carried out at 400 rpm. The kinetics are reported as mole fraction of aluminum reacted, *χ_{Al}*, based on the known total aluminum in the original kaolinite. The parameter *χ_{Al}* is used in the kinetic rate law expressions for film diffusion control, product layer diffusion control, and chemical reaction control. The experimental kinetic parameters are summarized in Table 2.

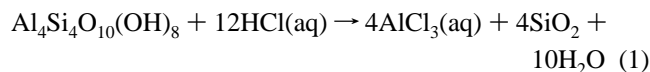
Solid-State ¹H CRAMPS Measurements. ¹H CRAMPS spectra were obtained at 187 MHz on a modified NT-200 spectrometer, using the BR-24 pulse sequence.^{36–38} The cycle time for the BR-24 pulse sequence varied between 108 and 144 μs, corresponding to a pulse spacing of 3.0–4.0 μs. Magic-angle spinning at 2.0–3.0 kHz employed a spinner based on the design of Gay.⁴⁰ Samples (ca. 10 mg) were sealed under vacuum in thick-walled 5 mm o.d. (2 mm i.d.) glass tubes. Repetition delays of 3–6 s and between 64 and 256 repetitions were used to obtain signal-to-noise ratios of at least 100/1.³¹ Chemical shifts

were referenced by sample substitution with tetrakis(trimethylsilyl)methane (TTMSM) and are reported relative to tetramethylsilane (TMS) at 0.0 ppm. The integrated intensities were obtained by deconvolution of the experimental spectra using Nicolet software. As the ¹H magnetization in the CRAMPS experiment is generated by a single-pulse preparation pulse, the intensities obtained from the ¹H CRAMPS spectra should accurately reflect quantitation for analytical purposes.

Solid-State ²⁹Si NMR Measurements. ²⁹Si NMR spectra were recorded on a "home-built" Nicolet NT-200 NMR spectrometer at 39.7 MHz (4.7 T). Samples were contained in ultravolume (2 cm³) Delrin spinners and spun at 1.8–2.2 kHz in a "home-built" probe.⁴⁰ The SP/MAS ²⁹Si NMR spectra, with high-power proton decoupling during the acquisition time, were obtained using observation ²⁹Si pulse tip angles of 30–70° and delay times from 250–600 s. Due to the large sample volume in the ultravolume spinners, only 16–24 scans with a 10 kHz sweep width were needed to obtain large signal-to-noise ²⁹Si NMR spectra. The ²⁹Si NMR spectra were externally referenced to tetrakis(trimethylsilyl)methane (TTMSM) assigned a chemical shift of 0.00 ppm (ca. −2 ppm lower than TMS). Since nonsaturating conditions were used, the intensities obtained from the deconvolution of the MAS ²⁹Si NMR spectra should be quantitative.

Results

Description of Dealuminated Kaolinite Solids. Dealuminated kaolinite solids used for the NMR experiments were obtained from the reaction of kaolinite with aqueous 3 M HCl at 98 °C for times of 4, 24, 48, 96, 192 (8 days), and 384 h (16 days) at a 10.79/1 HCl/kaolinite mole ratio corresponding to ca. 90% of the theoretical stoichiometry for complete reaction of the gibbsite-like Al(OH)₃ layer of kaolinite. The % Si



extracted reached 0.58%, whereas the % Al extracted varied from 1.66% (4 h) to 83.3% (16 days), paralleling the percent weight loss profile. The % Al removed for the dealuminated solids is summarized in Table 1. The Si/Al ratio of the dealuminated kaolinite solids increases from 1/1 to 10.37/1 after 16 days extraction (for analytical details, see ref 31).

X-ray powder diffraction was used to monitor the dealuminated kaolinite solids. Partially dealuminated materials exhibited the normal diffraction lines for kaolinite (e.g., the intense lines at 2θ values of 12.3° (7.2 Å) and 24.8° (3.59 Å)), the peak intensities decreasing in proportion to the degree of dealumination.

SP/MAS and CP/MAS ²⁹Si NMR of Dealuminated Kaolinite Solids. The CP/MAS ²⁹Si NMR spectra for the series of dealuminated kaolinite solids following HCl extraction over the various time periods have been previously reported³¹ and reveal as many as three peaks at ca. −89, −100, and −109 to −112 ppm. In addition, a weak signal at −84 to −85 ppm is obtained for solids following 96–384 h of HCl reaction (61% to 83% dealumination). Previous variable contact time studies³¹ showed that the relative peak intensities are significantly dependent on contact times with the polarization transfer rates

(40) Gay, I. D. J. *Magn. Reson.* **1984**, 58(3), 413.

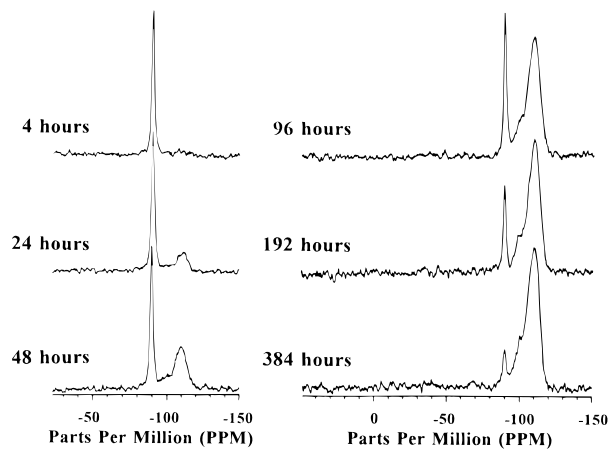


Figure 1. SP/MAS ^{29}Si NMR spectra (39.7 MHz and 1.8–2.2 kHz sample-spinning speed) for dealuminated kaolinite solids. Extraction in 3 M HCl for up to 384 h at 98 °C.

decreasing for the ^{29}Si peaks in the order –99, –89, and –109 ppm, indicating that the protons are nearer to the silicon atoms associated with the former two resonances. The two signals at –99 and –109 ppm are due to new silicon sites where the local chemical environment is altered as a result of the dealumination process.

The SP/MAS ^{29}Si NMR spectra and related ^{29}Si NMR chemical shifts and relative peak intensities for the dealuminated solids are summarized in Figure 1 and Table 1, respectively. The SP/MAS ^{29}Si NMR spectra of the partially dealuminated kaolinite solids reveal the same NMR peaks as found in the CP/MAS spectra. The sharp –89.1 to –90.9 ppm signal is assigned to Q^3 -type $\text{Si}(\text{OSi})_3(\text{OAl})_2$ sites, where each silicon has two second nearest-neighbor octahedral aluminums from the nearby aluminum hydroxide layer of unreacted kaolinite.⁴¹ The broader –99 peak (–96 to –102 ppm), with the fastest cross-polarization transfer rate, is assigned to newly formed Q^3 -type silicon sites with one second nearest-neighbor aluminum, consistent with assignments by Lippmaa *et al.* for zeolites and aluminosilicates^{42,43} and by Smith *et al.*⁴¹ for layered aluminosilicates. (The Q^n notation used by Lippmaa^{42,43} and Smith³⁹ regarding framework aluminosilicates and zeolites to provide a correlation between δ (^{29}Si) values and the chemical environments of silicons in Si/Al materials is not clearly applicable to clays in spite of its extensive usage for such assignments. For clay minerals like kaolinite, for example, the $\text{Si}(\text{OSi})_3(\text{OAl})_2$ sites are assigned a Q^3 notation due to arguments based on the occurrence of no second nearest-neighbor four-coordinate Al atoms, yet, two second nearest-neighbor six-coordinate Al atoms are present (Figure 4A).) The broadest signal at –110 ppm (–108 to –115 ppm), which has the slowest cross-polarization transfer rate, is assigned to newly formed Q^4 -type $\text{Si}(\text{OSi})_4$ sites of amorphous silica-like regions in these dealuminated solids.^{41–43}

The sum of the relative signal intensities of the –89 and –99 ppm peak regions can be correlated with the % Al remaining in the dealuminated kaolinite solids on the basis of comparison with the chemical analysis results shown in Table 1. These results provide evidence for the assignment of the –99 ppm resonance to new Q^3 -type $\text{Si}(\text{OSi})_3(\text{OAl})$ sites. For example, at 24 h HCl reaction (82.4% Al remaining), the sum of the relative intensities of the –89 ppm (63%) and –99 ppm peaks

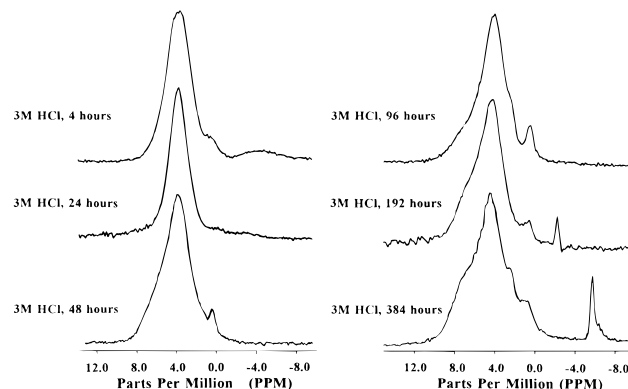


Figure 2. ^1H CRAMPS spectra (187 MHz) for dealuminated kaolinite solids. Extraction in 3 M HCl for up to 384 h at 98 °C.

(15%) is 78%; at 96 h (39.1% Al remaining), the sum of the relative intensities of the –89 ppm (22%) and –99 ppm peaks (18%) is 40%; at 384 h (16.7% Al remaining), the sum of the relative intensities of the –89 ppm (6%) and –99 ppm peaks (16%) is 22%. This quantitative relationship between the relative intensities of the SP/MAS ^{29}Si NMR resonances in the –89 and –99 ppm regions and the % Al remaining in these solids suggests that these resonances are principally associated with two silicon atom sites that have local chemical environments with nearby octahedral aluminum atoms that remain after the dealumination reaction. The –89 ppm resonance is assigned (*vide supra*) to the silicon atoms in the unreacted kaolinite, which are unaltered following the HCl extraction, whereas the latter NMR signal at –99 ppm is due to new silicon atom sites produced during the HCl(aq) reaction and that are in the vicinity of the unextracted octahedral second nearest-neighbor aluminum atom.

^1H CRAMPS Studies of Dealuminated Kaolinite Solids.

The ^1H CRAMPS spectra of the dealuminated kaolinite solids are shown in Figure 2. The ^1H CRAMPS spectrum of normal kaolinite (data not shown) exhibits a single broad resonance at 3.4 ppm, its spectrum being virtually identical to the 4 h dealuminated kaolinite solid (Figure 2). This resonance is assigned to the hydroxyl protons of the gibbsite-like aluminum hydroxide layer of kaolinite.

The ^1H CRAMPS spectra of the various dealuminated solids following 24–384 h HCl(aq) reaction show a broad resonance in the 3.4–4.1 ppm range due to the Al–OH–Al moiety of kaolinite and up to three new proton NMR peaks: (1) a less intense, sharper resonance at 0.2–0.5 ppm, (2) a shoulder at 2.3–2.5 ppm, and (3) a less intense, broad shoulder resonance at ca. 6.7–7.0 ppm. In addition, the narrow lines at about –2 ppm and –6 ppm in the ^1H NMR spectra of the 192 and 384 h dealuminated samples are due to rotor lines, a common feature of spectra for lossy samples. The ^1H CRAMPS peak at 3.4–4.1 ppm is assigned to a range of chemically different (at least three) protons in the Al–OH–Al moiety of unreacted kaolinite. The large resonance line width is in part due to chemical shift dispersion, as well as ^1H – ^{27}Al dipolar coupling. ^1H – ^{27}Al dipolar line-broadening effects have been previously noted by Bronnimann³⁵ in ^1H CRAMPS studies of alumina–silicas, by Freude *et al.*⁴⁴ in MAS ^1H NMR studies of zeolite H-ZSM-5, by Cholli and Pennino⁴⁵ in studies of natural mordenites, and by Freude *et al.*⁴⁶ in studies of alumina–silicas. The proton NMR peak at 3.4–4.0 ppm in kaolinite is observed to narrow

(41) Smith, K. A.; Kirkpatrick, R. J.; Oldfield, E.; Henderson, D. M. *Am. Mineral.* **1983**, *68*, 1206.

(42) Lippmaa, E.; Mägi, M.; Samoson, A.; Tarnak, M.; Engelhardt, G. *J. Am. Chem. Soc.* **1981**, *103*(17), 4992.

(43) Lippmaa, E.; Mägi, M.; Samoson, A.; Engelhardt, G.; Grimmer, A. R. *J. Am. Chem. Soc.* **1980**, *102*(15), 4890.

(44) Freude, D.; Klinowski, J. *J. Chem. Soc., Chem. Commun.* **1988**, 1411.

(45) Cholli, A. L.; Pennino, D. *J. Spectrosc. Lett.* **1987**, *20*(1), 25.

(46) Freude, D.; Hunger, M.; Pfeifer, H.; Scheler, G.; Hoffman, J.; Schmitz, W. *Chem. Phys. Lett.* **1984**, *105*, 427.

and shifts from 3.4 to 4.0 ppm for dealuminated kaolinite solids, presumably due to removal of adjacent aluminum atoms. The decreased line width of this peak is probably a result of the decrease in the ^1H – ^{27}Al dipolar coupling. The sharper 0.2–0.5 ppm peak, which initially appears following 4 h reaction and which is most readily resolved in the spectrum of the 96 h dealuminated solid is assigned to residual non-hydrogen-bonded "isolated" silanol (Si–OH) groups. The intensity of this resonance is relatively constant even as the percent dealumination increases up to 83.3% Al removal, reaching 45.8% of the relative proton population at 384 h. Bronnimann *et al.*³⁷ have previously observed "isolated" non-H-bonded silanols at 1.7 ppm in silica gels at various stages of hydration.

The broader shoulder resonance at 6.8–7.0 ppm is observed in all solids reacted for at least 48 h and is most intense in the 384 h dealuminated solid. The intensity of this new proton resonance increases with the degree of dealumination and is assigned to Si–OH⁺–Al groups. Bronnimann *et al.*³⁶ have previously reported proton-containing acidic Si/Al Brønsted sites in silica/alumina catalysts at 7.0 ppm, and Freude *et al.*⁴⁶ have assigned a 7.0 ppm peak to similar Si–OH⁺–Al sites in studies of silica–alumina. In the work reported here on dealuminated kaolinite, the Si–OH⁺–Al group contains six-coordinate aluminum based on the ^{27}Al NMR (no four-coordinate peak) and ^{29}Si NMR results, whereas in the studies of the alumina–silicas noted above, the more highly acidic Al–OH⁺–Si groups contain reported four-coordinate aluminums as is usually observed in such acidic catalytic sites for zeolites as well as alumina–silicas.

The ^1H CRAMPS peak, observed as a discernable shoulder at 2.3–2.5 ppm in the 48, 96, and 384 h dealuminated kaolinite solids, is assigned to "physisorbed" water. The intensity of this resonance is very dependent on sample preparation and can be eliminated following evacuation of the solid samples at 10×10^{-3} Torr for several hours. ^1H CRAMPS resonances for water "physisorbed" onto silica gels (at 3.1 ppm) and γ -alumina (at 4.8 ppm) have been reported^{36,37} and have been likewise eliminated by analogous sample evacuation procedures. It should be noted that the presence of the "physisorbed" water ^1H NMR peak, together with the other ^1H CRAMPS peaks at ca. 0.2–0.5 ppm and 6.8–7.0 ppm, indicates that these water protons are not in a fast chemical exchange process with these other proton-containing sites.

Semiquantitative analysis of the relative proton populations of two kaolinite solids has been obtained for evacuated samples obtained following 96 and 384 h reaction. For the kaolinite solid that is 60.9% dealuminated after 96 h, the percent relative intensities of the 0.4, 4.0, and 7.0 ppm ^1H CRAMPS peaks are 6.5%, 77%, and 16.1%, respectively. Similarly, for the kaolinite solid obtained following 384 h reaction and 3–4 h evacuation, the percent relative signal intensities are 4.2%, 50.0%, and 45.8% for the 0.5, 4.1, and 6.9 ppm peaks, respectively. These results indicate that the relative proton population of the residual silanol (Si–OH) groups produced following the HCl(aq) extraction reaction is essentially independent of reaction time. The formation of acidic Si–OH⁺–Al proton sites, however, increases as kaolinite is dealuminated, concomitant with a decrease in the percent relative intensity of the proton sites in the Al–OH–Al structural unit of unreacted kaolinite.

Theoretical Model of Kaolinite–HCl Reaction. The reaction of kaolinite with HCl(aq) has been described as a "heterogeneous" process that may involve mass transport of reactant and product ions and chemical reactions at the solid/solution interface. The kinetics of the reaction of kaolinite with stoichiometric aqueous HCl according to eq 1 were analyzed

in terms of a shrinking unreacted core model as described by Livenspiel⁴⁷ for heterogeneous fluid–particle reactions. The overall process involves three steps: (i) diffusion of hydrogen ions through a mass transfer boundary layer, (ii) diffusion of hydrogen ions through a product solid layer, and (iii) chemical reaction of hydrogen ions at the interface between unreacted and completely reacted zones. The rate-determining step is determined by the slowest process. Analysis of the rate law expression is based on three assumptions: (i) the reaction is irreversible, (ii) kaolinite particles are spherical, and (iii) the shape and size of the kaolinite particles are unchanged following acid extraction of aluminum. Han *et al.*⁴² have reported kinetic studies for the reaction of ilmenite (FeTiO₃) with aqueous sulfuric acid solutions between 88 and 115 °C, which used the following three integrated rate law equations for the three processes:

(1) **film diffusion control**, where diffusion through the mass transfer boundary layer is rate-determining, as given by the equation

$$\chi_{\text{Al}} = K't, \text{ where } K' = (3 Vb k_m C_b)/r_o \text{ and } b = 1/12 \quad (2)$$

(2) **product layer diffusion control**, where diffusion of reactant through a product layer or residual layer is rate-limiting, as given by the equation

$$K't = 1 - 3(1 - \chi_{\text{Al}})^{2/3} + 2(1 - \chi_{\text{Al}}), \text{ where } K' = (6VbD_e C_b)/r_o^2 \quad (3)$$

(3) **chemical reaction control**, where the rate of consumption of the reactant hydrogen ion and formation of the product layer is proportional to the area of the unreacted core of the particle, as given by equation

$$K't = 1 - (1 - \chi_{\text{Al}})^{1/3}, \text{ where } K' = (Vb k_s C_b^n)/r_o \quad (4)$$

The various parameters in these equations are defined as follows: b = stoichiometric reaction coefficient, n = order of reaction with respect to C_b , $C_b = [\text{H}^+]$ in bulk solution, V = molar volume of kaolinite, χ_{Al} = the mole fraction of aluminum reacted or extracted, r_o = average initial radius of the kaolinite particle, k_m = rate constant for the mass transfer reaction, k_s = rate constant for the chemical reaction, t = time, and D_e = effective diffusion coefficient of hydrogen ions in a porous medium. The progress of the reaction is unaffected by the presence of a product layer in a chemical reaction-controlled process. Equations 2–4 predict that χ_{Al} has a characteristic time dependence that is dependent on which of the three processes considered controls the rate of reaction. Thus, measurements of χ_{Al} as a function of time should permit the rate-controlling step of the reaction to be determined.

Experimental Dealumination Kinetics. The rate of release of Al^{3+} ion into solution, $d[\text{Al}]/dt$, during the reaction of kaolinite with HCl(aq) at 98 °C and a 12:1 kaolinite/HCl stoichiometry, was obtained as a function of the kaolinite particle size, the concentration of HCl(aq), and the temperature in order to determine which of the possible steps in the reaction, eqs 2–4, is the rate-determining step. Once the functional form of K' is known, the rate constant (k_s) and the activation energy of the reaction can be calculated.

Figure 3A shows a plot of $1 - (1 - \chi_{\text{Al}})^{1/3}$ versus time for four different kaolinite particle sizes; this plot clearly demonstrates that the initial rate of reaction of kaolinite with HCl(aq) is under chemical control for reaction times up to 192 h, according to eq 4. These data also show that the effective rate constant K' decreases as r_o increases, as predicted by eq 4,

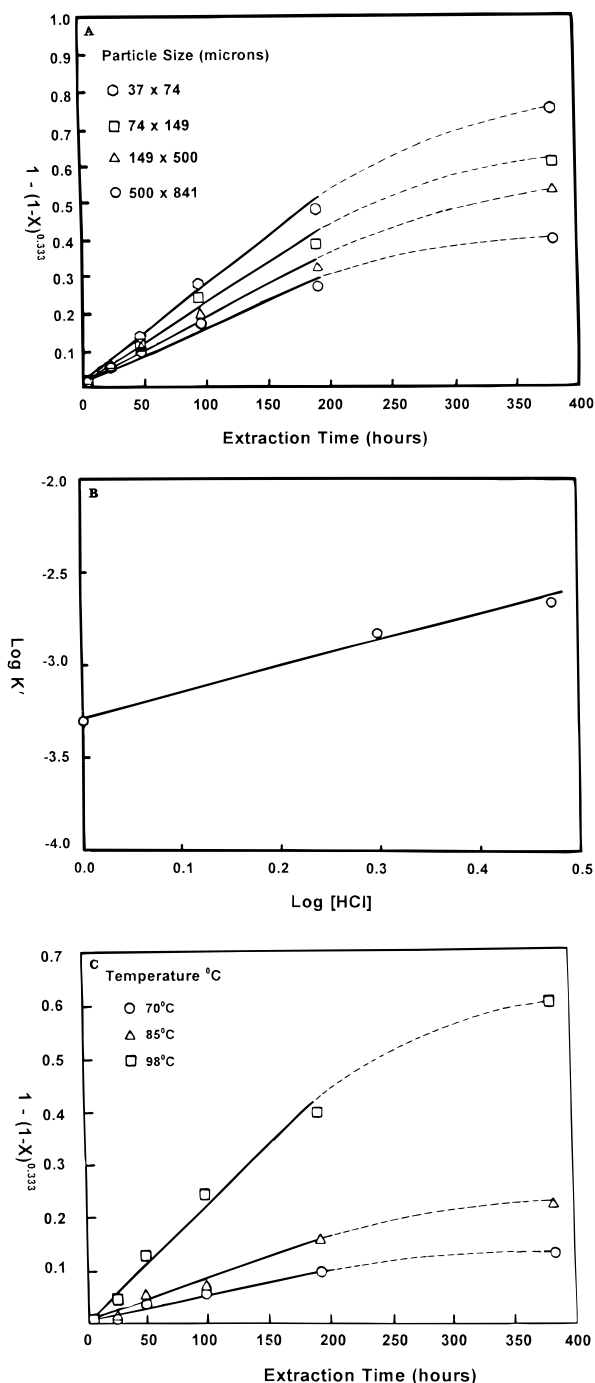


Figure 3. (A) Plot of $1 - (1 - \chi)^{1/3}$ versus time for different kaolinite particle sizes. Conditions: 3 M HCl, 98 °C, and 400 rpm. (B) Plot of $\log K'$ versus $\log [\text{HCl}(\text{aq})]$. Conditions: 149 \times 500 μm , 98 °C, 400 rpm. (C) Plot of $1 - (1 - \chi)^{1/3}$ versus time at different temperatures. Conditions: 149 \times 500 μm , 3 M HCl, and 400 rpm.

consistent with the use of the shrinking unreacted core model⁴⁷ to describe the reaction of kaolinite with HCl(aq). In addition, eq 4 shows that the order of reaction with respect to the mole fraction of aluminum in kaolinite is two-thirds, a result that contradicts the earlier work of Miller³² (see below). A summary of the experimental kinetic rate constants K' and k_s , obtained at the various reaction conditions, is given in Table 2.

Similar plots of $1 - (1 - \chi_{\text{Al}})^{1/3}$ versus reaction time (not shown) were also obtained for the reaction of kaolinite (149 \times 500 μm range) at three [HCl] conditions: 1.0, 2.0, and 3.0 M

at 98 °C. The effective rate constants for the reaction at these various [HCl] conditions are given in Table 2. From a plot of $\log K'$ versus $\log [\text{HCl}(\text{aq})]$ (Figure 3B), the order of the reaction with respect to [HCl(aq)] at 98 °C was determined to be $n = 1.3$.

With this value of n , the rate constant describing the initial rate of the chemically-controlled reaction, k_s , is obtained using the expression $K' = (Vbk_s C_b^n)/r_0$. These k_s values are summarized in Table 2 for the various reaction conditions. The average K' and k_s values obtained from the four different particle sizes at 3 M HCl and 98 °C are $1.99 \times 10^{-3} \text{ h}^{-1}$ and $3.51 \times 10^{-5} \text{ cm h}^{-1}$, respectively.

Figure 3C shows plots of $1 - (1 - \chi_{\text{Al}})^{1/3}$ versus reaction time for the reaction of kaolinite (particle size 149 \times 500 μm) with 3 M HCl as a function of temperature. The effective rate constant K' increases as the temperature increases. The rate constants K' and k_s obtained from these data are summarized in Table 2. The activation energy (E_a) determined from the temperature dependence of the rate constant is $E_a = 52.2 \text{ kJ/mol}$. This value of E_a also supports a chemically-controlled process; Habashi⁴⁹ has shown that $E_a < 10 \text{ kJ/mol}$ for a diffusion-controlled process through a liquid boundary, while $E_a > 42 \text{ kJ/mol}$ for a chemically-controlled process. Similarly, Han⁴⁸ has reported $E_a = 64.4 \text{ kJ/mol}$ for the chemically-controlled solid/solution reaction of ilmenite with concentrated aqueous H_2SO_4 in the temperature range 88–115 °C.

In summary, the order of the reaction with respect to [HCl(aq)] at 98 °C was 1.3 as determined by a plot of $\log K'$ vs $\log [\text{HCl}(\text{aq})]$ as given in Figure 3B. A plot of K' vs $[\text{HCl}(\text{aq})]^{1.3}$ was found to be linear with a zero intercept and a correlation coefficient of 0.99. The rate constant for the chemically-controlled reaction was calculated using eq 4 to be $6.8 \times 10^{-6} \text{ cm min}^{-1}$. The overall rate equation for the dealumination of kaolinite in aqueous HCl was $d[\text{Al}]/dt = 6.8 \times 10^{-6} [\text{HCl}(\text{aq})]^{1.3}$, where $d[\text{Al}]/dt$ is the rate of appearance of aluminum in solution.

Discussion

Chemical Model of Dealuminated Kaolinite Solids. The chemical structure of kaolinite consists of an $\text{Al}(\text{OH})_3$ -like gibbsite layer linked via Si–O–Al groups to the silica layer as shown in Figure 4A. Solid-state MAS ^{27}Al NMR reveals a single resonance at 5.1 ppm³¹ due to the six-coordinate aluminum, although two nonequivalent aluminums are present.^{1,2} The structure of kaolinite also consists of two nonequivalent silicon atoms. Barron et al.⁵⁰ and Thompson⁵¹ have observed two ^{29}Si NMR peaks for a pure mineral-quality specimen of kaolinite, and Jocha and Klinowski⁵² have recently reported similar results. Generally, only a single ^{29}Si NMR peak at -89 to -92 ppm due to the Q³-type Si(OSi)₃(OAl)₂ sites is observed. The ^1H CRAMPS spectrum of kaolinite shows a broad resonance at 3.4 ppm, which arises in part from a range of chemical shifts due to a range of chemically distinct (at least three) proton sites in the Al–OH–Al moieties. In addition, the large resonance line width has a significant contribution from ^1H – ^{27}Al dipolar coupling as previously noted.³¹

A structural model of dealuminated kaolinite, where 60% of the aluminums (and associated $\text{Al}(\text{OH})_3$ layer) have been

(48) Han, K. N.; Rubcumintara, T.; Fuerstenau, M. C. *Metall. Trans. B.* **1987**, *18B*, 325.

(49) Habashi, F. *Principles of Extractive Metallurgy*; Gordon and Breach: New York, 1969; Vol. 1, pp 153–163.

(50) Barron, P. F.; Raymond, L. F.; Skjemstad, J. O.; Koppi, A. J. *Nature* **1983**, *302*, 49.

(51) Thompson, J. G. *Clays Clay Miner.* **1984**, *32*, 233.

(52) Rocha, J.; Klinowski, J. *J. Magn. Reson.* **1990**, *90*, 567.

(47) Levenspiel, O. *Chemical Reaction Engineering*, 2nd ed.; John Wiley and Sons: New York, 1972; pp 357–377.

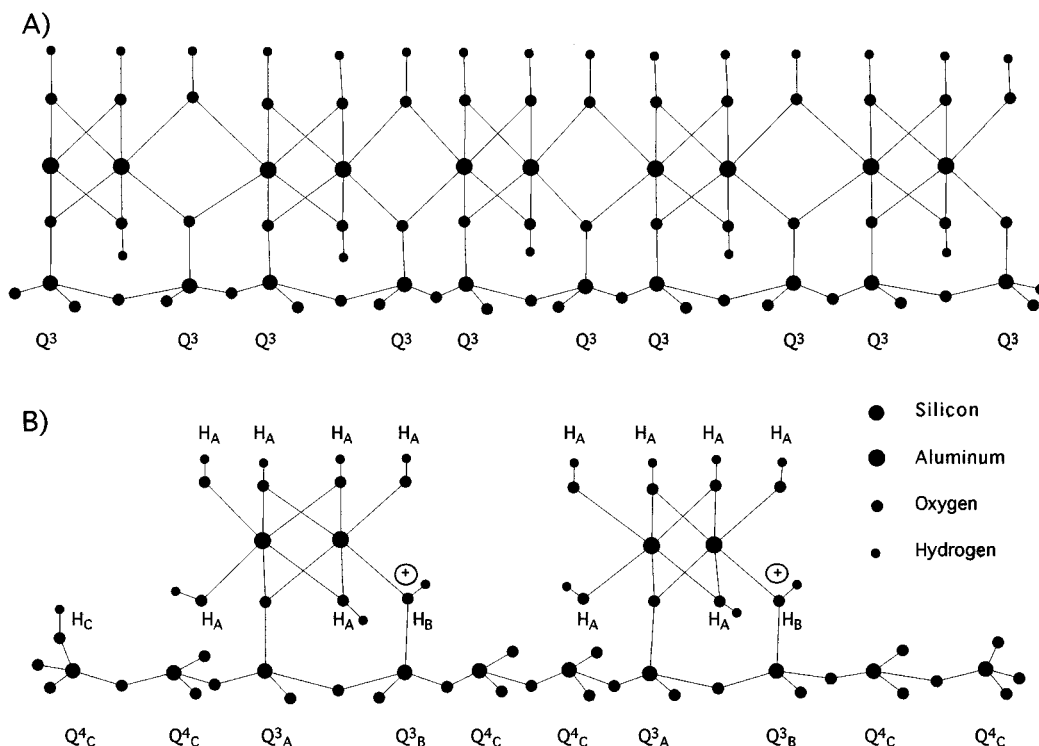


Figure 4. Schematic depiction of structural models of (A) kaolinite and (B) 60% dealuminated kaolinite.

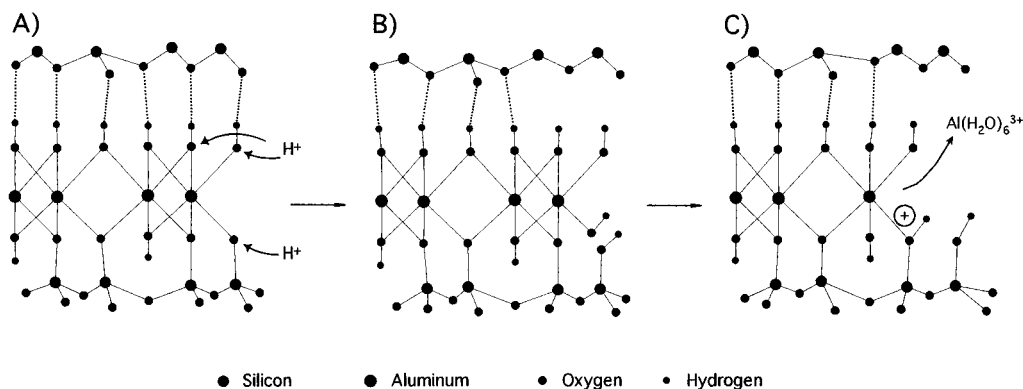


Figure 5. Plausible mechanism of H^+ ion edge attack of kaolinite and subsequent liberation of $Al(H_2O)_6^{3+}$ ion.

removed, is given in Figure 4B. The proposed model is based on 1H , ^{27}Al , and ^{29}Si NMR results for the dealuminated kaolinite solids studied here and elsewhere³¹ following reaction for 96 h in $HCl(aq)$ (60.9% dealuminated). The model contains the following structural features: (1) the coordination of the aluminum atoms is essentially identical to those in the original $Al-OH-Al$ layer of kaolinite, (2) the silica layer consists of four distinctly nonequivalent silicon atoms (Si_A-Si_D), and (3) the structure contains three nonequivalent proton sites (H_A-H_C), a proton associated with the silanol in the silica layer (H_C), a proton in the vicinity of a silicon atom corresponding to the new interface $Si-OH^+-Al$ moiety (H_B), and one (H_A) corresponding to a range of $Al-OH$ or $Al-OH-Al$ groups in the intact segments of the gibbsite-like layer that are not removed by reaction with $HCl(aq)$.

The results obtained from the MAS ^{27}Al NMR³¹ indicate that the local structure of aluminums in partially dealuminated kaolinite solids is similar to that of unreacted kaolinite. The proposed structural model is consistent with these results and reflects the fact that 60% of the Al atoms have been removed from the kaolinite.

The four silicon atom sites in the proposed structural model of 60% dealuminated kaolinite is also consistent with the SP/

MAS results reported here and the previous CP/MAS ^{29}Si NMR results.³¹ Quantitative SP/MAS ^{29}Si NMR measurements (Table 1) show that approximately 22%, 18%, and 60% of the silicons are associated with the -89 , -100 , and -110 ppm resonances, respectively. The Si_A sites at -89 ppm are similar to the original silicon atoms of the silica layer, the Si_B sites at -100 ppm are assigned to new $Si-OH^+-Al_{oh}$ sites of dealuminated solids, and the Si_C sites at -110 ppm are assigned to amorphous $Si(OSi)_4$ sites formed following dealumination. In addition, a minor Si_D site, which is assigned to residual non-hydrogen-bonded "isolated" Q^2 -type silanol groups ($Si(OSi)_2(OH)_2$ and is probably less than 5% of the silicons, is also included in the model and is consistent with deconvolution analysis of several ^{29}Si NMR spectra that showed a low-intensity resonance at -80 ppm. Excluding the minor Si_D site, the relative ratios of the three primary silicon sites ($Si_A:Si_B:Si_C$) is 2:2:6 based on the SP/MAS ^{29}Si NMR results and is consistent with a $Si_A:Si_B:Si_C$ ratio of 2:2:6 from the structural model of dealuminated kaolinite. An alternate model to that of Figure 5B, wherein all four aluminum octahedra in the remaining $Al(OH)_3$ layer are connected, was also considered. This structural model also consists of three primary silicon sites (Si_A-Si_C), in addition to the minor Si_D site. Excluding the minor Si_D site, the relative

ratios of the $\text{Si}_A:\text{Si}_B:\text{Si}_C$ populations is 3:2:5, which is not in agreement with the SP/MAS ^{29}Si NMR results. This alternate model may, however, represent some regions of the dealuminated kaolinite materials formed early in the reaction prior to the formation of a more highly porous 60% dealuminated material as found at 96 h.

The CP/MAS ^{29}Si NMR results reported previously³¹ are also consistent with these three primary types of silicon sites in dealuminated kaolinite. Previous contact time studies showed that the $^1\text{H}-^{29}\text{Si}$ cross-polarization is most favorable for the -100 ppm signal (Si_B), followed by the -89 ppm peak (Si_A) and then the -110 ppm signal (Si_C). These results are consistent with the relative number and proximity of the various adjacent protons to these three silicon sites.

The structural model of the 60% dealuminated kaolinite solid proposed is also qualitatively consistent with the ^1H CRAMPS spectrum of the 96 h dealuminated solid. Three major ^1H NMR resonances are observed (Figure 2) for this sample at 0.7, 3.4, and 6.8, which are assigned to new "edge" silanol group protons (site H_C , 6.5%), a range of protons in $\text{Al}-\text{OH}-\text{Al}$ or $\text{Al}-\text{OH}$ groups (site H_A , 77.4%), and protons in the new $\text{Si}-\text{OH}^+-\text{Al}_{\text{OH}}$ groups (site H_B , 16.1%), respectively. The relative intensity ratio of the H_A/H_B proton sites is ca. 4.8:1, while the relative proton ratio is 6:1 for these two sites in the proposed structural model. These results are in agreement with the semiquantitative nature of the ^1H NMR spectral intensities.

The ^1H CRAMPS and ^{29}Si NMR results are internally consistent since the ^{29}Si NMR peak at -100 ppm (Si_B) is assigned to the silicons of the newly formed $\text{Si}-\text{OH}^+-\text{Al}_{\text{OH}}$ groups. These silicon atoms are strongly coupled to the protons that are likely responsible for the ^1H CRAMPS peak at 6.8 ppm. Similarly, the original silicon (Si_A) sites of kaolinite are observed in the ^{29}Si NMR spectrum at -89 ppm and are more moderately coupled with numerous protons associated with the $\text{Al}-\text{OH}-\text{Al}$ layer in both kaolinite and the dealuminated kaolinite solids.

Kinetic Model of Dealumination of Kaolinite. The kinetics of dealumination of kaolinite in $\text{HCl}(\text{aq})$ may be considered from three primary perspectives: (1) the nature of the rate-limiting process of this two-phase solid/solution "interfacial" reaction, (2) the possible mechanisms of H^+ ion attack of the mineral, and (3) the mode of liberation of Al^{3+} ion from kaolinite into the solution medium.

The kinetic results reported here support a chemically-controlled reaction where the rate of consumption of H^+ ion is proportional to the size of the unreacted core of the kaolinite particles. The rate of the reaction is under chemical control up to 192 h, after which time the chemically-controlled rate law expression shows deviation. The rate of formation and association of released Al^{3+} product ions (e.g., $\text{Al}(\text{H}_2\text{O})_6^{3+}$ ion or hydrolysis products such as $\text{Al}_2(\text{OH})_2(\text{H}_2\text{O})_8^{4+}$) at the mineral surface due to decreased pH or collapse of the completely dealuminated silica layer regions of kaolinite particles at longer times may account for this deviation of the rate law expression from chemical reaction control at longer times. However, the rate-limiting process is consistent with studies by Miller,³² who showed that the liberation of Al^{3+} ion from kaolinite in excess acidic media is controlled by a rate-limiting chemical "interfacial" reaction. The rate law for this process reported by Miller³² was pseudo-zero-order with respect to aluminum in kaolinite under excess acid conditions (3.6×10^5 $\text{HCl}/\text{kaolinite}$ ratio). In the work reported here, the dealumination process is observed to be two-thirds order in aluminum and approximately pseudo-first-order with respect to H^+ ion at a 12:1 $\text{HCl}/\text{kaolinite}$ reaction ratio. Differences between the reaction order with

respect to H^+ ion reported here and the zero-order dependence reported by Miller³² are attributed to the high excess H^+ ion concentration used by Miller. An experimental rate law equation $d[\text{Al}]/dt = k[\text{H}^+]^n$, where $n = 1.3$ and the average $k_s = 3.51 \times 10^{-5}$ cm h^{-1} , was obtained in 3 M HCl at 98°C . The apparent activation energy of 52.2 kJ/mol is also consistent with a chemically-controlled reaction according to Habashi.⁴⁹

Two mechanisms of H^+ ion attack of the mineral surface are most plausible for this chemically-controlled "interfacial" reaction, an all-surface attack and an edge attack. Miller³² has proposed that an edge attack of kaolinite is consistent with the pseudo-zero-order kinetics of this reaction in excess acid, while an all-surface attack of montmorillonite by H^+ ion is consistent with pseudo-first-order kinetics. The basis for these differences is attributed to structural differences in these clays since kaolinite is a more closed structure than montmorillonite, which has available surface cavities for reaction, in addition to mineral surface edge reaction sites. The ^1H CRAMPS and SP/MAS ^{29}Si NMR and the structural model of dealuminated kaolinite reported here support the edge attack mechanism for liberation of Al^{3+} ion as proposed by Miller.³² In this mechanism, H^+ ion attack is postulated to initially occur by protonation of the an edge hydroxide group of an $\text{Al}-\text{OH}$ moiety that is hydrogen-bonded to the silica units of the adjacent layers as shown in Figure 5A. At least two hydrogen-bonded AlOH groups must be protonated to liberate one Al^{3+} ion. Next, protonation of the oxide of the $\text{Si}-\text{O}-\text{Al}$ linkage of the intact silica/alumina framework of the mineral is proposed as shown in Figure 5A. Rupture of the protonated $\text{Si}-\text{OH}^+-\text{Al}$ linkage by water attack with the formation of an edge silanol is probably the rate-limiting step (Figure 5B). Subsequent protonation of Al -coordinated hydroxide group to form coordinated water and generate a partially liberated $>\text{Al}(\text{H}_2\text{O})_4$ unit may be followed by protonation of the next hydrogen-bonded AlOH group and then acid hydrolysis of another $>\text{AlO}(\text{Al}(\text{H}_2\text{O})_5$ unit. Eventually, protonation of the coordinated hydroxide groups leads to $\text{Al}(\text{H}_2\text{O})_6^{3+}$ ion diffusion into solution (Figure 5C). Following liberation of $\text{Al}(\text{H}_2\text{O})_6^{3+}$ ion into solution, the partially dealuminated kaolinite consists of three key structural features that are consistent with the structural model of Figure 4B, residual mineral edge silanols, $\text{Si}-\text{OH}^+-\text{Al}$ moieties at the site of removal of a series of Al^{3+} ions, and amorphous silica regions formed following condensation of silanol groups in dealuminated regions of the kaolinite.

The proposed mechanism of dealumination may be visualized to occur not only along one plane of the kaolinite layers but also in two and three dimensions at all edge sites accessible to H^+ ion attack, consistent with a shrinking core kinetic model. Such a process is likely to produce a more open dealuminated structure as proposed in Figure 4B, indicating that the dealuminated solids are quite porous at later stages of dealumination as confirmed microscopically.

Conclusions

Solid-state ^1H CRAMPS and CP/MAS and SP/MAS ^{29}Si NMR techniques have been used to study dealuminated kaolinite solids prepared by the solid/solution "interfacial" reaction of kaolinite with aqueous HCl . ^1H CRAMPS results have identified three distinct proton sites that are contained in $\text{Al}-\text{OH}-\text{Al}$, $\text{Si}-\text{OH}^+-\text{Al}$, and $\text{Si}-\text{OH}$ moieties of dealuminated kaolinite, as well as protons due to "physisorbed" water. SP/MAS and CP/MAS ^{29}Si NMR measurements have identified three distinct silicon sites in dealuminated kaolinite, including new alumina-silica sites containing six-coordinate aluminums, amorphous silica sites formed in these mineral-derived solids

following removal of aluminum from the aluminum hydroxide layers, and the original Q³-type silicon sites of kaolinite. The relative contents of the proton sites from ¹H CRAMPS results and the silicon atom sites from SP/MAS ²⁹Si NMR measurements are markedly dependent upon the degree of dealumination. The solid-state ¹H CRAMPS and ²⁹Si NMR assignments have permitted the development of a chemical structural model for dealuminated kaolinite solids. Kinetic studies of this dealuminated reaction show that this solid/solution “interfacial” reaction is chemically-controlled, with the attack of H⁺ ion at the Si–O–Al linkages along the mineral edges being proposed as the rate-limiting reaction step to liberate Al³⁺ ion into solution. The simultaneous application of ¹H CRAMPS and

MAS ²⁷Al and ²⁹Si NMR techniques to examine this mineral suggests new avenues for future investigations of solid/liquid interfacial reactions important for a wide range of layered clay minerals and other well-defined layered inorganic materials.

Acknowledgment. The authors gratefully acknowledge the Colorado State University Regional NMR Center, funded by National Science Foundation Grant No. CHE9021003, for use of their excellent NMR facilities. One of the authors (J.J.F.) acknowledges partial support of this work by the National Science Foundation Grant Nos. RII-8902066 and OSR-9108773. JA970305M